RSC Advances

This is an *Accepted Manuscript*, which has been through the Royal Society of Chemistry peer review process and has been accepted for publication.

Accepted Manuscripts are published online shortly after acceptance, before technical editing, formatting and proof reading. Using this free service, authors can make their results available to the community, in citable form, before we publish the edited article. This *Accepted Manuscript* will be replaced by the edited, formatted and paginated article as soon as this is available.

You can find more information about *Accepted Manuscripts* in the Information for Authors.

Please note that technical editing may introduce minor changes to the text and/or graphics, which may alter content. The journal's standard Terms & Conditions and the Ethical guidelines still apply. In no event shall the Royal Society of Chemistry be held responsible for any errors or omissions in this *Accepted Manuscript* or any consequences arising from the use of any information it contains.

ROYAL SOCIETY OF CHEMISTRY

www.rsc.org/advances

Stretchable CNT-interlayered PDMS Sheet

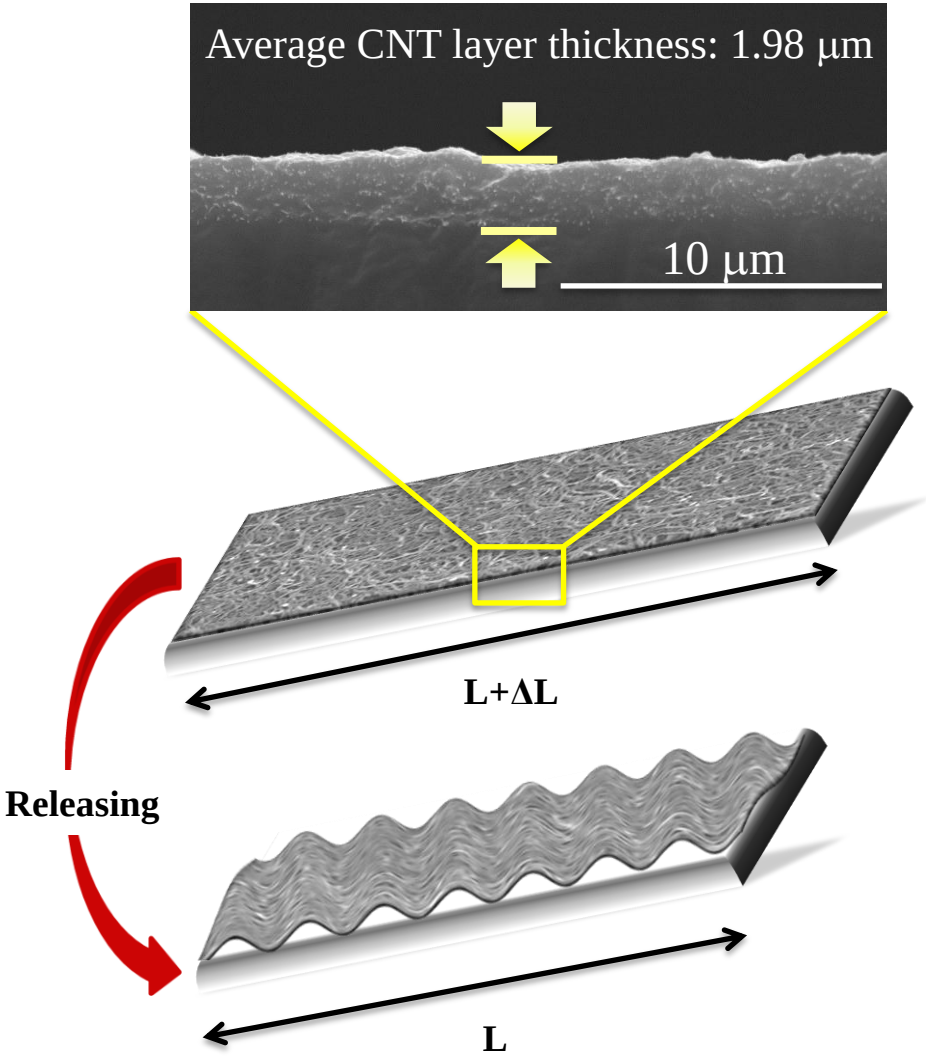

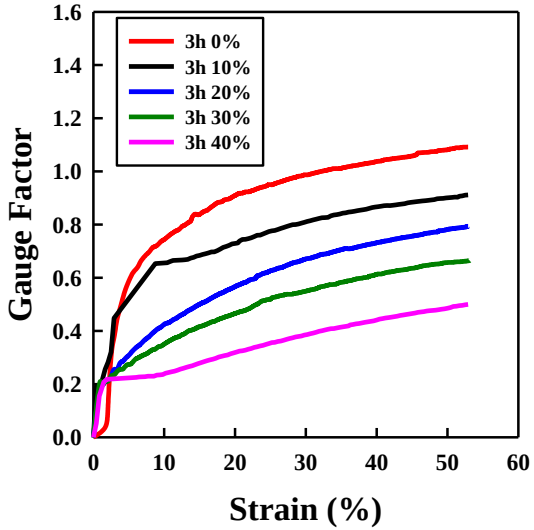

RSC Advances Accepted Manuscript

Journal Name

ARTICLE

Piezoresistive Behavior of a Stretchable Carbon Nanotube-Interlayered Poly(dimethylsiloxane) Sheet with a Wrinkled Structure

Received 00th January 20xx,
Accepted 00th January 20xx

DOI: 10.1039/x0xx00000x

www.rsc.org/

Joonhoo Jung, Kyung Min Lee, Sung-Hyeon Baeck and Sang Eun Shim*

Piezoresistive behavior of a stretchable poly(dimethylsiloxane) sheet with a interlayer of carbon nanotube in it (CNT-interlayered PDMS) was investigated based on two variables: indivisual length of CNT which forms interlayer and degree of pre-tension of the sample during the preparation stage. The stress-strain curves exhibited good stretchable properties of the CNT-interlayered PDMS sheets, similar to that of neat PDMS sheets and better than that of CNT/PDMS composites. The electrical resistance changed almost linearly with applied strain and the results of piezoresistive experiments evidenced that these two variables are factors that indeed affect piezoresistive behavior. The results are explained by the pre-tension-derived wrinkled structure of the CNT layer and the effect of ultrasonication on the CNT length. The sensitivity is described by a gauge factor in the range 0.19–1.16. The samples show good conductivity even at large elongations (~55 %) and excellent properties in cyclic piezoresistive experiments at small (~11 %) as well as at large strain.

1. Introduction

The piezoresistive effect means a change in the electrical resistivity of materials in dependence of an applied mechanical force. It is distinct from the piezoelectric effect that changes the electrical potential because it changes only the electrical resistance. Since Thomson first reported on the change in resistance upon elongation in iron and copper in 1856,[1] a great deal of effort has been made for determining the change in resistance under applied stress.[2-9] In 1935, Cookson first mentioned the term "piezoresistive effect" ("piezo" is derived from the Greek word piezein, which means to squeeze or press).[10]

The piezoresistive effect has been mostly investigated in materials that are based on composites of conductive fillers and polymer matrices.[11-15] Especially, among the conductive fillers, CNTs have attracted a great deal of attention owing to their unique and versatile properties, since multi-walled carbon nanotube (MWCNT) and single-walled carbon nanotubes (SWCNT) were discovered by Ijima in 1991 and Bethune et al. in 1993, respectively.[16,17] Dang et al. presented piezoresistive properties of MWCNT/silicone rubber nanocomposites with different aspect ratio. A high aspect ratio of MWCNT made the composites more sensitive to pressure.[18] Olivia-Aviles et al. reported on alignment of MWCNT in polysulfone that resulted in improved electrical and piezoresistive sensing capabilities of the composite film.[19]

Department of Chemistry & Chemical Engineering, Inha University
253 Yonghyundong, Namgu, Incheon, 402-751 Republic of Korea.
E-mail: seshim@inha.ac.kr

Recently, stretchable, foldable, and deformable conductive materials have been researched for various applications such as in the biomedical field,[20,21] as electronic paper[22] in human motion detection sensors,[23] and in photovoltaics.[24,25] In order to achieve a superior performance in these diverse applications, the systems require lightweight and a sturdy construction using thin, flexible, stretchable, and electrically conductive materials. However, technical difficulties for embodying the desired characteristics into the composites still exist. New structural configurations are proposed as possible solutions. One of them is to fabricate wavy (wrinkled or buckled) conductive structures on an elastic substrate. The wavy structure enables a battery electrode to elongate without decrease in conductivity,[26] thereby retaining its electrochemical properties after 2,000 stretching cycles at 30 % of applied strain.[27] The conductor can be stretched much beyond the fracture strain of a free- standing conductive film on an elastomer substrate.[28] Another way is to take advantage of conductive materials with a large aspect ratio or in the liquid state to keep them conductive under tensile stain.[29,30]

Several researchers used different methods for CNT coating on various substrates at the laboratory scale. Dip coating, which is a simple process that provides a great potential to be scaled up for large-scale coating, was used for making colloid-regulated CNT networks.[31] Ng et al. introduced an adhesion promotor to overcome the problem of hydrophobicity and the consequent lack of adhesion exhibited by CNT during the process of dip coating.[32] Electrostatic spray deposition was employed by Kim et al. for preparing a CNT film onto a metallic substrate. This method has several advantages such as its ability for preparation of a binder-free CNT film electrode with

RSC Advances Accepted Manuscript

a uniform film-surface morphology, easy control of film mass and thickness, and a low operating temperature.[33]

Here we produced stretchable and durable CNT-interlayered PDMS sheets by spray coating because of some particular virtues, namely it is a simple and swift method and enables to regulate the transparency easily. Moreover, we achieved a new structural configuration by cover coating the electrode with an elastomer. Before considering application aspect, the outstanding characteristics of stretchable CNT-interlayered PDMS sheets were revealed by several experiments, such as observing the CNT-layer thickness on the PDMS substrate, determining the elongation properties, including the Young's modulus. The superior mechanical properties of CNT-interlayered PDMS sheets are especially remarkable if compared to CNT/PDMS composites and pristine PDMS sheets. The piezoresistive properties are investigated with respect to two variables, namely the ultrasonication time and the degree of pre-strain applied to the substrate in the sample preparation step. In particular, the results of piezoresistivity experiments are explained in terms of micro- (CNT size) and macro-scale structures (CNT layer structure). Finally, a gauge factor (GF) and repetitive stretching and releasing experiments are also presented.

2. Experimental

2.1. Materials

PDMS (Mw = 600,000 g mol^{-1}, 0.03 mol % of vinyl groups) and the cross-linking agent 2,5-dimethyl-2,5-di(tert-butylperoxy)hexane (DHBP) (AkzoNobel, Netherlands) were supplied by Grace Continental, South Korea. MWCNT (NanocylTM NC 7000, average diameter of 9.5 nm and length of 1.5 μm) was purchased from Nanocyl (Belgium). Liquid-type silicone elastomer and the curing agent for cover-coating were purchased from Dow Corning (South Korea).

2.2 Preparation of CNT-interlayered PDMS sheets

First, pure PDMS sheets were fabricated by using a laboratory two-roll mill (Daekyung Engineering Co., S. Korea). DHBP (1 phr) was added as a cross-linking agent to PDMS. Then, the sheets were compression molded under 0.98 MPa at 170 °C. The prepared PDMS sheets were cut in a rectangular shape with 2 cm in width and 8 cm in length. The procedure used for preparing stretchable CNT-interlayered PDMS is illustrated in Fig. 1(b). The PDMS substrate was uniaxially stretched from 100 % to 140 % of the initial length and a CNT dispersion was prepared by sonicating a mixture of 0.1 g of MWCNT and 100 g of ethanol in an ice bath using an ultrasonic liquid processor model SH-750S (Sonictopia, S. Korea) at 20 kHz. The probe type sonicator was operated in pulse operation mode (on 2 s, off 1 s) and the power was set at 187.5 W (intensity: 78.72 W/cm^2). We varied the effective sonication time from 1 h to 3 h. CNT thin films were produced

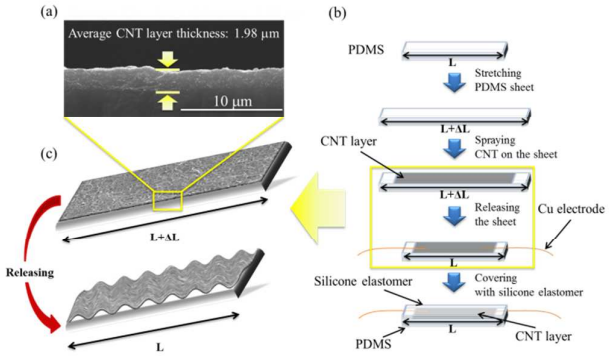

Fig. 1 (a) SEM image of the CNT layer between substrate and cover and (b) schematic illustration of the concept of achieving wrinkled structures of the CNT layer on the substrate when releasing the sample, and (c) the procedure for preparing CNT-interlayered PDMS sample.

by deposition of the MWCNT dispersion on the PDMS substrate using the spray-coating method with an Iwata spray gun W-61. 10 times of spraying were conducted for 3 sec each in the distance of 200 mm between PDMS substrate and nozzle which has 1.0 mm of fluid nozzle orifice and 0.29 MPa of atomizing air pressure. Releasing the pre-strained substrate leads the CNT layer to develop wrinkled structures perpendicular to the elongation direction, shown in Fig. 1(c). Two electrodes were attached at the both ends of a CNT layer with silver paste for electrical conductivity measurements. Uncured silicone elastomer was spread onto the CNT-sprayed PDMS sheet for fabricating the cover-coating on top of the CNT layers in sequence. Note that the silicone elastomer cover-coating enhances the originally poor adhesion between CNT and PDMS and protects the CNT layer from mechanical scratching. Last, the sample was baked in an oven at 120 °C for 45 min to cure the silicone elastomer, finally resulting in CNT-interlayered PDMS sheets. For the purpose of comparison, CNT/PDMS composite films were prepared with same way with CNT-interlayered PDMS sheets, excepting that CNT was mixed with raw PDMS before cross-lingking agent.

2.3. Characterization

SEM micrographs were obtained by a Hitachi S-4300 microscope (Japan). The SEM was performed for examining the thickness and surface morphology of the CNT layers. The samples were fractured in liquid nitrogen and sputter-coated with platinum prior to the SEM characterization. TEM micrographs were acquired by a Philips CM200 (USA). The TEM was used for investigating the CNT length in the CNT dispersions which were sonicated for 1 h, 3 h, and 5 h. The dispersions were dried in a vacuum oven at 60 °C before the TEM analysis. The CNT-interlayered PDMS sheets in dumbbell geometry were tested for determining the tensile properties, such as the Young's modulus. The tensile tests were conducted using a universal testing machine (UTM, Instron 5569, USA) at an elongation rate of 50 mm min-1 at room temperature. The CNT-interlayered PDMS sheets with rectangular geometry mentioned above were examined under uniaxial elongation for their piezoresistive characterization. The electrical resistance

RSC Advances Accepted Manuscript

This journal is © The Royal Society of Chemistry 20xx

was measured using a FLUKE 289 True-rms Logging Multimeter (USA) while the sheets were elongated at rate of 5 mm min-1 by UTM. In a repetitive stretching and releasing experiment, the sample was pulled for 5 min and then returned to the initial position. After 5 min, the next cycle was started.

3. Results and discussion

3.1. Characterization of CNT-interlayered PDMS sheet

3.1.1. Thickness of the CNT layer

Fig. 1(a) shows the scanning electron microscopy (SEM) image of a vertical section of the CNT layer on the substrate. It reveals that the layer has a very good uniformity in thickness that explains that the CNTs are evenly deposited on the substrate by spray coating. The average thickness was found to be around 1.98 μm.

3.1.2. Genuine properties of CNT-interlayered PDMS sheets

The stress–strain (S–S) curve and Young's modulus were measured to fully understand outstanding property of CNT-layered sheet. Fig. 2(a) shows that there is a conspicuous difference between raw PDMS and CNT/PDMS composites sheet, even between the composites with 2 phr and 4 phr CNT.

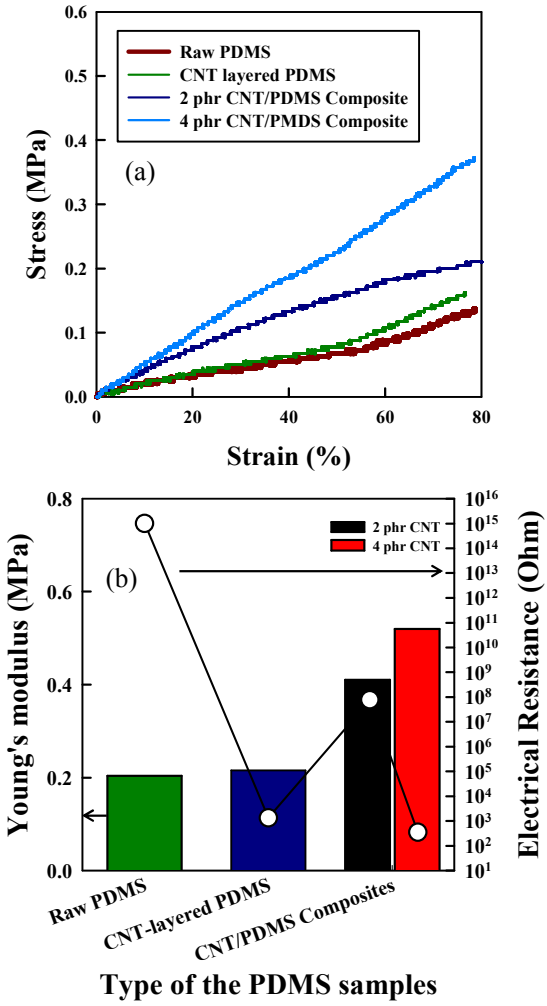

Fig. 2 (a) Stress–strain curves and (b) Young's moduli of raw PDMS, CNT-interlayered PDMS , and CNT/PDMS composite (2 phr and 4 phr).

However, the CNT-interlayered PDMS has a much similar S–S curve with the raw PDMS rather than with the CNT/PDMS composite sheets. This means that the tensile property of the CNT-interlayered PDMS sheets is close to pristine PDMS sheets. Furthermore, in order to illustrate excellent properties of the CNT-interlayered PDMS sheets, the Young's modulus and the electrical resistance of all samples are plotted together in Fig. 2(b). The bars indicate the Young's moduli, and the straight line shows the electrical resistance. First of all, we compare the Young's modulus among raw PDMS, CNT-interlayered PDMS, and CNT/PDMS composite sheets. Regardless of the electrical resistance, the Young's modulus of the CNT-interlayered PDMS sheet is similar with that of the raw PDMS sheet, in contrast to the 2 phr CNT/PDMS composite sheet that has a significantly higher Young's modulus. Second, considering the electrical resistance, we added more CNT filler into the composite to reach a similar degree of the electrical resistance of CNT-interlayered PDMS sheet which has a value of around 10^3 Ω (see Supporting Information Fig. S1). As a result, although the Young's modulus of the composite sheets is already greater than that of the CNT-interlayered PDMS sheets, it leads to a further increase in the Young's modulus for the 4 phr CNT/PDMS composite sheets. Several researches conform this increasing rigidity on increasing filler content.[13,34] The CNT-interlayered PDMS sheet retains virtues of both materials which are a great electrical conductivity of pure CNT and a softness of pristine PDMS without any significant change in other properties. Therefore, the CNT-interlayered PDMS has a great potential to be applied in various fields.

3.2. Piezoresistive property

3.2.1. Electrical resistance variation in dependence of elongation

Fig. 3 presents the relative resistance (R/R_0) as a function of strain (~55%). Although it is clear that the strain has an influence on the resistivity, however, the focus of this experiment is the effect of sonication time and pre-strain which affect the variation of the relative resistance on strain. The variation of the relative resistance becomes larger when the sonication time increases and, reversely, it becomes smaller when the degree of pre-strain increases. We explain this phenomenon based on scale of size (micro or macro). First of all, at the macro scale, the main effect originates from the wrinkled structure of the CNT layer which is also the reason that the sample is a stretchable conductive material. To support this, we observed the surface of a CNT layer on the PDMS substrate by SEM, shown in Fig. 4.

There is a noticeable discrepancy of the wrinkling length which apparently decreases as the pre-tension increases from 10 % to 40 %. Fig. 5 shows the average wrinkling length of the CNT layer. From these data, we derived the relationship that a shorter wrinkling length implies a larger number of CNT layer wrinkles on the substrate which, in turn, allows the samples to withstand longer elongations until all the wrinkles are

RSC Advances Accepted Manuscript

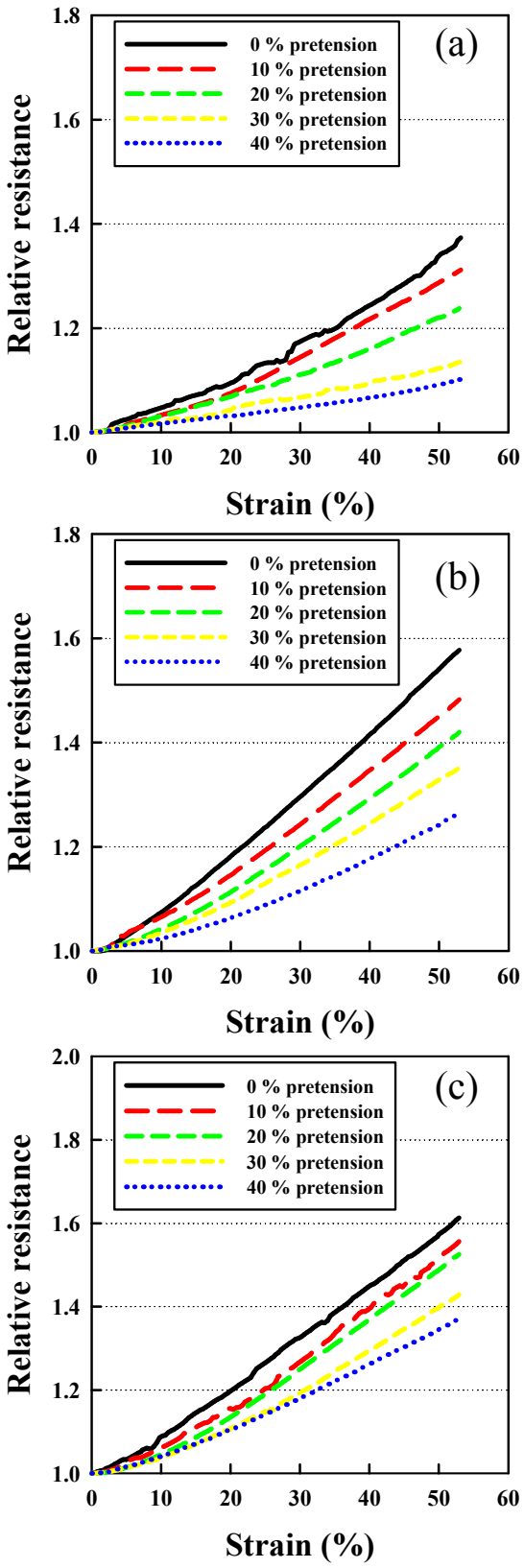

straightened. Therefore, the variation of the relative resistance changes only gently because the CNT conductive paths remain without failure by the elongation. The linear increase in resistivity was explained by the fracturing mechanism of CNT film.[35] Irreversible fracturing by stretching forms CNT islands and gaps between them connected by small CNT bundles. Further stretching creates more number of CNT islands and larger gap distance. Second, at the microscale, the variation in the relative resistance is due to the difference in CNT length, induced by sonication.

Fig. 3 The relative resistance as a function of strain for various pre-tension levels and different sonication times of (a) 1 h, (b) 3 h, and (c) 5 h.

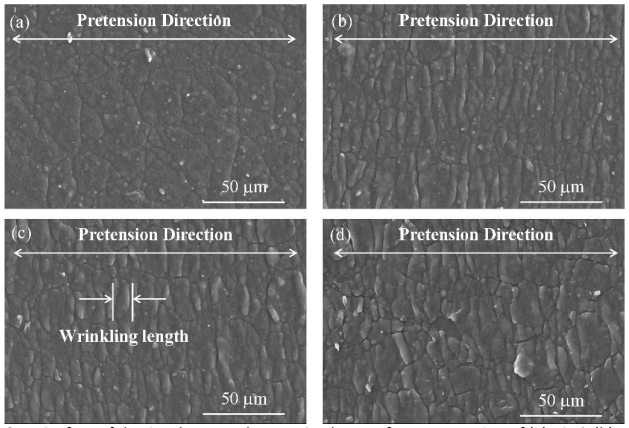

Fig. 4 Surface of the CNT layer on the PDMS substrate for a pre-tension of (a) 10 %, (b) 20 %, (c) 30 %, and (d) 40 %.

To prove more evidence, we analyzed CNT dispersions that were sonicated for 0, 1, 3, and 5 h by transmission electron microscopy (TEM), whose images are displayed in Fig. 6. The average CNT lengths and the standard deviations are listed in Table 1 and indicate a decreasing length of CNT as well as standard deviation on increasing sonication time. There are a few reports about the sonication effect on the CNT length. Lucas et al. studied the kinetics of nanotube and microfiber scission under sonication. They measured the average MWCNT length by dynamic light scattering to diminish any possible undesirable alternation in the data and observed that the applied acoustic energy influences the scission speed.[36]

Hacht et al. investigated the bundle length and diameter of SWCNT, treated by sonication for 1–1,000 min, by atomic force microscopy and reported on the noticeable fact of decreasing average bundle length and diameter of the SWCNT up on longer sonication times.[37]

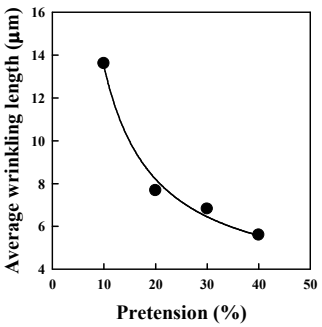

RSC Advances Accepted Manuscript

This journal is © The Royal Society of Chemistry 20xx

Fig. 5 The average wrinkling length of the surface of CNT-interlayered PDMS with pre-tension.

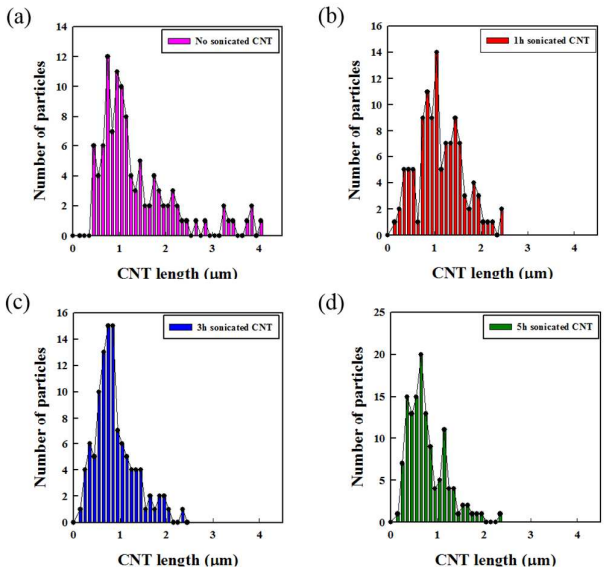

Fig. 6 The effect of sonication on the CNT particle size and the corresponding equivalent particle-size distribution for sonication times of (a) 0 h , (b) 1 h, (c) 3 h, and (d) 5 h.

Although, of course, there could be an error in the determing CNT length determined by TEM microscopes, we are convinced the fact that the tendency of a decreasing CNT length is a dependable result, because the average CNT length on the basis of TEM of the CNT dispersion without sonication effect, shown in Fig. 6(a), is similar to that of raw CNT provided from the supplier, namely 1.4 μm and 1.5 μm, respectively. In turn, the reason why the CNT length is the most crucial factor is the number of remaining junctions which play an important role in the development of conductive paths.

Long CNTs can maintain more junctions than short CNTs on applied strain. In other words, the junctions of the short CNTs are easily detached from others if the elongation of the sample is beyond the length of the CNT, at least.

Fig. 7 presents the GF which is the standard for quantifying the piezoresistive sensitivity, as stated above.

Table 1. Reduction in the length of multi-walled carbon nanotubes treated by ultrasonication

Sonication time (h)	Mean length (μm)	Standard deviation
0	1.41	0.83
1	1.18	0.49
3	0.94	0.43
5	0.82	0.40

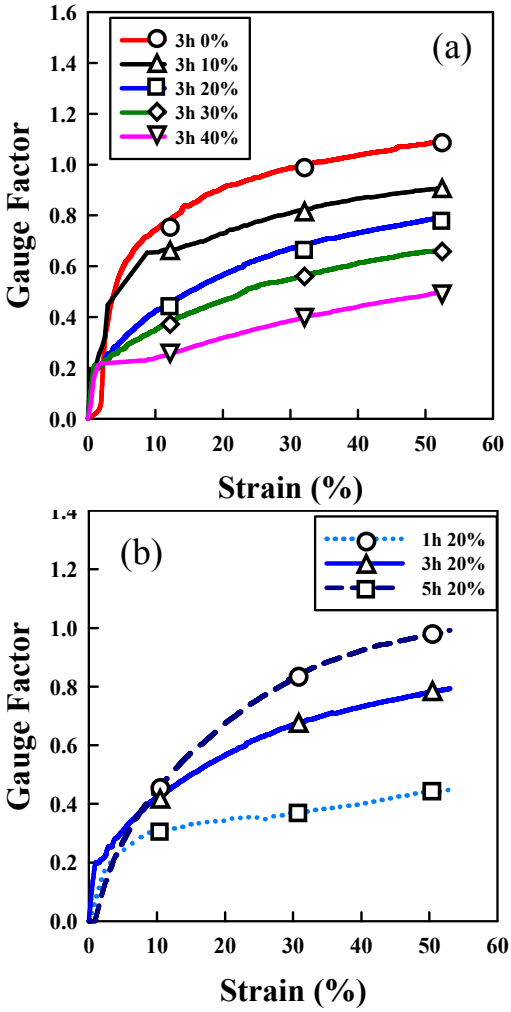

Fig. 7 Gauge factors as a function of applied strain of samples (a) with various degrees of pretension and (b) with various lengths of sonication time.

It is determined on the basis of elongation experiments, by using the following equation:

$$\mathrm{GF} = \frac{\Delta \mathrm{R} / \mathrm{R}_0}{\Delta l / l_0} = \frac{\Delta R}{\varepsilon R_0} \qquad (1)$$

Here, Δ*R* and Δ*l* are the changes in the electrical resistance and the elongation length, respectively ($\Delta \mathrm{R} = \left| \mathrm{R} - \mathrm{R}_0 \right|, \Delta l = \left| l - l_0 \right|$). R_0 and l_0 are the initial values of the resistance and the length, respectively. The GF is also affected by the sonication time and the degree of pre-tension. In Fig. 7(a), the GF is shown for various pre-tension degrees at a fixed sonication time. The highest value of GF is 1.09 without pre-tension and the lowest value is 0.49 for 40 % pre-tension of the sample. In Figure 7(b), the GF for diverse sonication times at the same level of pre-tension of 20 %. The sensitivity of the sample is larger for

RSC Advances Accepted Manuscript

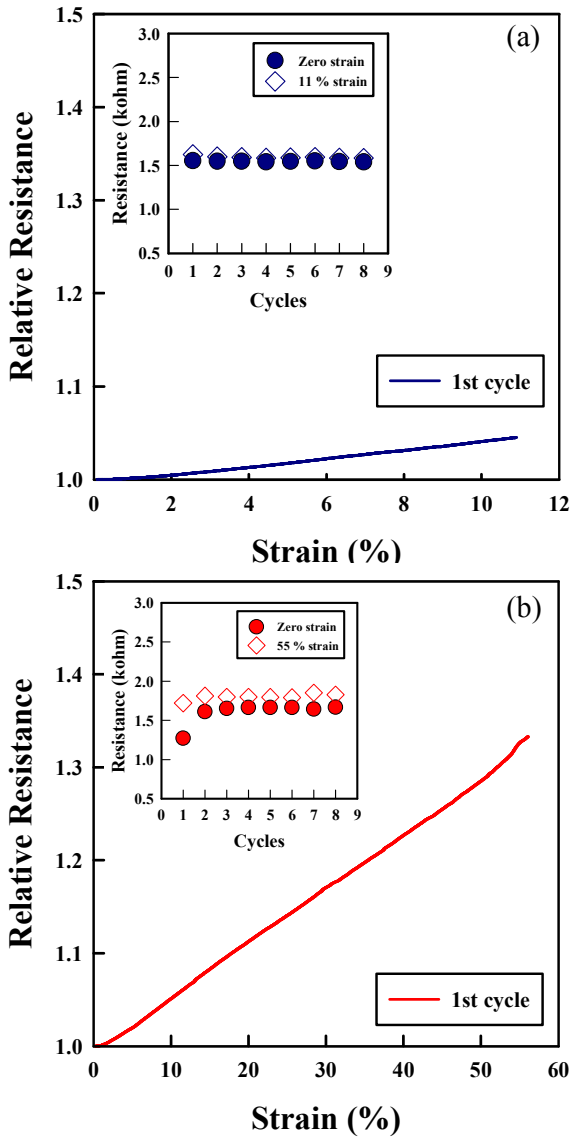

Fig. 8 Repeatability test for small strain (a) and large strain (b) (1h 20% pre).

longer sonication times. With these results, we can conclude that a long sonication time and a small degree of pre-tension are favorable for the making of a more sensitive sample.

However the important point of the present study is to know how sensitive the CNT-interlayered PDMS sheets are when comparing to alternative composites or other forms of piezoresistive materials. In the case of rubber composites, a large GF is observed due to the large elasticity. It allows rubber composites for a big deformation which is related to a change in electrical resistance. The GF of MWCNT/PDMS composites varied from 1.38 to 12.4 in dependence of various CNT loadings,[14] and that of carbon black/PDMS composites was determined to be about 7.4.[38] On the other hand, plastic-based composites have less sensitivity than rubbers.

A SWCNT/polyimide composite has a GF value of 4.21 and that GF of SWCNT/PMMA composite films increased from 1 to 5.2 when the CNT content decreased from 10 wt% to 0.5 wt%.[39] Considering semiconductors, n-type β-SiC has a GF of 31.8 (absolute value).[39] It is noted that none of the above cases are stretchable. The CNT-interlayered PDMS has a GF in the range from 0.19 (1 h sonication time and 40 % pre-tension of the sample) to 1.16 (5 h sonication time and no pre-tension), similar to metal foils. It means that the sample has two advantages, namely maintenance of good conductivity during elongation and an operable piezoresistive sensitivity.

3.2.3 Repetitive piezoresistive behaviour

Fig. 8 presents the results of repetitive piezoresistive experiments for 1 h of sonication of the CNT-interlayered PDMS samples. Two ranges of strain, small (11 %) and large (55 %), were applied for these experiments. We observed a slight change in the relative resistance during the first measurement of the small-strain repetitive experiment, shown in Fig. 8(a).

It was verified that the following measurements were not different from first one, as evidence in the inset of Fig. 8(a). However, a large deviation in the relative electrical resistance was observed, especially between the first and the second measurement, in the large-strain repetitive experiment shown in Fig. 8(b). This phenomenon is also observed in other samples (see Figure S2 for the effect of pre-tension on the repeatability). The main reason is that the deformation of the substrate remained, which is a characteristic features of rubber known as “set”. In other words, when the stress is removed, the unstrained state is not attained immediately. Because of the set, the sample has different dimensions when starting the first and the second cycle. The deformation, of course, could be restored after a sufficient time due to the elasticity of rubber, but it takes 10 min for conducting one cycle of the experiment that is not enough for that the sample regain its original length. In spite of this result, the sample shows a very good repeatability and sustains a high conductivity.

4. Conclusions

By developing CNT layers on the PMDS sheets and covering the materials with a silicone elastomer, we fabricated structurally sturdy and stretchable CNT-interlayered PDMS sheets. The electromechanical and piezoresistive properties of these sheets were characterized. On the basis of these experiments, three noticeable characteristics have been found. First, the poor adhesion between the CNT and PDMS surface can be improved and the sample is protected against any environmental influence by the cover-coating of the silicone elastomer. Second, the sheets are stretchable and remain conducting under large tensile and compressive strains until failure. Third, it is easy to control their electro-mechanical properties as compared to other composites. The composites have some advantages in that their properties can be controlled by changing the filler type and content, and the type of polymer matrix. However, any change in one of these parameters has a great effect on the composite properties. For

RSC Advances Accepted Manuscript

This journal is © The Royal Society of Chemistry 20xx

example, the increasing rigidity of the composite, owing to the addition of fillers for improved electrical conductivity, cannot be avoided. In these respects, this hybrid structure of CNT-interlayered PDMS sheets has a remarkable virtue in that it can give not only the electrical conductivity of carbon but also the flexibility and stretchability of PDMS without significant influence on each other's properties. There are differences in the variation of the relative electrical resistance among the samples with varied length of sonication times and degrees of pre-tension. The sonication time for the CNT dispersion influences the piezoresistivity owing to decreasing CNT length, which in effect reduces the remaining number of junctions in the conductive paths up on elongation. The pre-strain of the samples also affects the results because of the wrinkling that allows the samples to withstand elongation. In other words, the samples maintained a high conductivity even at high elongation levels. By controlling the sonication time and the pre-strain, the GF could be also modulated without difficulty. Although the sensitivity of CNT-interlayered PDMS sheets is relatively lower than that of other forms of carbon materials, the sample has two virtues. One is the value of the piezoresistive GF that is suitable for various applications and the other is higher electrical conductivity than that of alternative piezoresistive composites. Although a small deviation in the relative resistance obtained through various measurements in cyclic tests was observed at 11% strain, and a relatively large deviation was observed at 55% strain, the sample exhibited good repeatability.

Acknowledgements

This work was supported by National Research Foundation of Korea (grant no.: 3148213322).

Notes and references

1 W. Thomson, *Proc R Soc London*, 1856, **8**, 546-550.
2 H. Tomlinson, *Proc R Soc London*, 1876, **25,** 451-453.
3 H. Tomlinson, *Philos Trans R Soc London*, 1883, **174**,171-172.
4 P. Bridgman, *Proc Natl Acad Sci USA*, 1924, **10,** 411-415.
5 P. Bridgman, *Proc Am Acad Arts Sci*, 1925, **60,** 423-449.
6 H. Rolnick, *Phys Rev*, 1930, **36,** 506-512.
7 M. Allen, *Phys Rev*, 1932, **42,** 848-857.
8 M. Allen, *Phys Rev*, 1933, **43,** 569-576.
9 M. Allen, *Phys Rev*, 1937, **52,** 1246-1249.
10 J. W. Cookson, *Phys Rev*, 1935, **47**, 194-195.
11 W. Luheng, D. Tianhuai and W. Peng, *Carbon*, 2009, **47**, 3151-3157.
12 S. Luo and T. Liu, *Carbon*, 2013, **59**, 315-324.
13 M. K. Abyaneh and S. K. Kulkarni, *J Phys D*, 2008, **41**, 135405-135411.
14 J. Lu, M. Lu, A. Bermak and Y. Lee, *presented at 7th IEEE Conf Nanotechnol,* Hong Kong, China, August*,* 2007.
15 J. H. Kang, C. Park, J. A. Scholl, A. H. Brazin, N. M. Holloway, J. W. High, S.E. Lowther and J. S. Harrison, *J Polym Sci Part B: Polym Phys,* 2009, **47**, 994-1003.
16 S. Ijima, *Nature*, 1991, **354**, 56-58.
17 D. S. Bethune, C. H. Klang, M. S. de Vries, G. Gorman, R. Savoy, J. Vazquez and R. Beyers, *Nature*, 1993, **363**, 605-607.
18 Z. M. Dang, M. J. Jiang, D. Xie, S. H. Yao, L. Q. Zhang and J. Bai, *J Appl Phys*, 2008, **104**, 024114-024114-6.
19 A. Oliva-Avilés, F. Avilés and V. Sosa, *Carbon,* 2011, **49**, 2989-2997.
20 R. Carta, P. Jourand, B. Hermans, J. Thoné, D. Brosteaux, T. Vervust, F. Bossuyt, F. Axisa, J. Vanfleteren and R. Puers, *Sens Actuators A*, 2009, **156**, 79-87.
21 Z. Yu, O. Graudejus, C. Tsay, S. P. Lacour, S. Wagner and B. Morrison III, *J Neurotrauma*, 2009, **26**, 1135-1145.
22 D. H. Kim, Y. S. Kim, J. Wu, Z. Liu, J. Song, H. S. Kim, Y. Y. Huang, K. C. Hwang and J. A. Rogers, *Adv Mater*, 2009, **21**, 3703-3707.
23 T. Yamada, Y. Hayamizu, Y. Yamamoto, Y. Yomogida, A. Izadi-Najafabadi, D. N. Futaba and K. Hata, *Nat Nanotechnol,* 2011, **6**, 296-301.
24 Y. Sun, W. M. Choi, H. Jiang, Y. Y. Huang and J. A. Rogers, *Nat Nanotechnol,* 2006, **1**, 201-207.
25 J. Yoon, A. J. Baca, S. I. Park, P. Elvikis, J. B. Geddes III, L. Li, R. K. Kim, J. Xiao, S. Wang, T. H. Kim, M. J. Motala, B. Y. Ahn, E. B. Duoss, J. A. Lewis, R. G. Nuzzo, P. M. Ferreira, Y. Huang, A. Rockett and J. A. Rogers, *Nat Mater,* 2008, **7**, 907-915.
26 M. Watanabe, H. Shirai and T. Hirai, *J Appl Phys,* 2002, **92**, 4631-4637.
27 C. Wang, W. Zheng, Z. Yue, C. O. Too and G. G. Wallace, *Adv Mater,* 2011, **23**, 3580-3584.
28 S. P. Lacour, S. Wagner, Z. Huang and Z. Suo, *Appl Phys Lett,* 2003, **82**, 2404-2406.
29 S. Cheng, A. Rydberg, K. Hjort and Z. Wu, *Appl Phys Lett*, 2009, **94**, 144103 - 144103-3.
30 H. Kim, C. Son and B. Ziaie, *Appl Phys Lett,* 2008, **92**, 011904 - 011904-3.
31 M. H. Kim, J. Y. Choi, H. K. Choi, S. M. Yoon, O. O. Park, D. K. Yi, S. J. Choi and H. J. Shin, *Adv Mater*, 2008, **20**, 457.
32 M. H. A. Ng, L. T. Hartadi, H. Tan and C. H. P. Poa, *Nanotechnology*, 2008, **19**, 205703-205705.
33 J. H. Kim, K. Nam, S. B. Ma and K. B. Kim, *Carbon,* 2006, **44**, 1963-1968.
34 D. Beruto, M. Capurro and G. Marro, *Sens Actuators A,* 2005, **117**, 301-308.
35 T. Yamada, Y. Hayamizu, Y. Yamamoto, Y. Yomogida, A. Izadi-Najafabadi, D. N. Futaba, and K. Hata, *Nat. Nanotechnology*, 2011, **6**, 296-301
36 A. Lucas, C. Zakri, M. Maugey, M. Pasquali, P. van der Schoot and P. Poulin, *J Phys Chem C,* 2009, **113**, 20599-20605.
37 D. Hecht, L. Hu and G. Gruner, *Appl Phys Lett*, 2006, **89**, 133112-133113.
38 M. Lu, A. Bermak and Y. Lee, *presented at 20th Int. Conf. MEMS.*, Kobe, Japan , January 2007.
39 I. Kang, M. J. Schulz, J. H. Kim, V. Shanov and D. Shi, *Smart Mater Struct*, 2006, **15**, 737-748.
J. S. Shor, D. Goldstein and A. Kurtz, *IEEE Trans Electron Dev* 1993, **40**, 1093-1099.

RSC Advances Accepted Manuscript